

Reflectance spectra of ZnCr_2Se_4 spinel from 4 to 100 eV measured
with synchrotron radiation: Band structure, covalency,
and final-state interactions

S. Suga, S. Shin, M. Taniguchi, K. Inoue, and M. Seki
*Synchrotron Radiation Laboratory, Institute for Solid State Physics,
The University of Tokyo, Tanashi, Tokyo 188 Japan*

I. Nakada and S. Shibuya
Institute for Solid State Physics, The University of Tokyo, Roppongi, Minatoku, Tokyo 106, Japan

T. Yamaguchi
Department of Applied Physics, Faculty of Engineering, Shizuoka University, Hamamatsu 432, Japan
(Received 13 July 1981)

Reflectance spectra of a ZnCr_2Se_4 single crystal have been measured in the wavelength region from 3000 to 120 Å. Final-state interactions of the $M_{2,3}3p$ inner-core excited states of the Cr^{3+} ion have been quantitatively evaluated from the analysis of the multiplet structures in the x-ray ultraviolet (xuv) spectrum on a basis of a recently developed ligand-field theory. The vacuum ultraviolet (vuv) reflectance spectra of the spinel are interpreted for the first time by taking into account the results of band calculations and the covalency effect.

I. INTRODUCTION

Among various transition-metal chalcogenide spinels, the chromium spinels $M\text{Cr}_2X_4$ (M represents Zn, Cd, and Hg; X represents S, Se, and Te) have been most extensively investigated because of their unusual optical, electrical, and magnetic properties.^{1,2} In order to interpret such properties in terms of microscopic mechanisms based on their electronic structures, a considerable amount of work has been performed on band calculations,^{3,4} elucidating details of the valence, as well as conduction, bands. Meanwhile, an extended measurement of the vuv reflectance spectrum of CdCr_2Se_4 has been performed up to 12 eV.⁵ Such results of optical measurements may serve as a check on the results of band calculations with respect to the top and bottom of valence and conduction bands as well as various bands in a wide energy range. When one measures optical spectra in the xuv region, one can observe inner-core transitions corresponding to constituent individual atom. By virtue of the small dispersion and localized character of the core levels, one can obtain much information about covalency and final-state interactions as well as band parameters through the analysis of the inner-core optical spectra.

As for the $3p$ core states of the chromium ion in transition-metal compounds, absorption spectroscopy has been performed on chromium halides and

has revealed multiplet structures of the $M_{2,3}$ absorption spectrum.^{6,7} In order to avoid the problem of stoichiometry in the case of absorption measurements for evaporated thin films of chemically unstable materials, we have carried out reflectance measurements on a single crystal of chromium chalcospinel. Within various chromium chalcospinels, we employed ZnCr_2Se_4 for the present study, which is a normal spinel with nonmagnetic Zn^{2+} ions. ZnCr_2Se_4 becomes antiferromagnetic below about 20 K, and susceptibility measurements at higher temperatures show an asymptotic Curie temperature to be 115 K.^{2,8} The spiral spin ground state suggests that at least one of the distant-neighbor interactions is ferromagnetic. In order to obtain a comprehensive understanding of the electronic structures of chromium chalcospinels, we have measured vuv reflectance spectra (above 400 Å) as well as xuv spectra (below 500 Å) of ZnCr_2Se_4 .

II. EXPERIMENTAL

We measured reflectance spectra of ZnCr_2Se_4 from natural surfaces of a single crystal grown by the chemical vapor deposition (CVD) method, which is similar to the standard method described elsewhere.⁹ As the starting material for the crystal preparation, sintered powder of ZnCr_2Se_4 was

pressed into a pellet and put in a quartz ampoule with a transport agent CrCl_3 . The evacuated and sealed ampoule was placed in a horizontal furnace with a temperature gradient. The pellet was placed at one end of the ampoule where the temperature was kept at 850°C . Tiny single crystals grew at the other end of the ampoule kept at 800°C for about a week. A crystal with a specular surface thus obtained with dimensions of about $2 \times 3 \text{ mm}^2$ enabled us to measure good reflectance spectra. SOR-RING, a 400-MeV electron storage ring of the Synchrotron Radiation Laboratory, Institute for Solid State Physics, was used as a light source for the measurements. Reflectance spectra were measured in the wavelength region from 120 to 3000 \AA by use of a sodium salicylate-coated window or light pipe and a photomultiplier. In particular, a plane-grating grazing-incidence monochromator was used between 120 and 500 \AA , and a Seya-Namioka monochromator was used between 400 and 3000 \AA . Typical resolution of these monochromators was set to 1 and 4 \AA , respectively. For the measurements in the former wavelength region, a grazing-incidence reflectivity was measured at an incidence angle of $\alpha = 45^\circ$ for *s*-polarized light, instead of measuring the near-normal incidence reflectivity for *p*-polarized light performed in the latter wavelength region. For the measurements performed with the Seya-Namioka monochromator, we employed several filters, such as LiF or MgF_2 single crystals and fused quartz, in order to reduce the effect of second-order light and to check the content of stray light.

III. RESULTS

Figure 1 shows the xuv reflectance spectrum of ZnCr_2Se_4 for *s*-polarized light measured at $\alpha = 45^\circ$

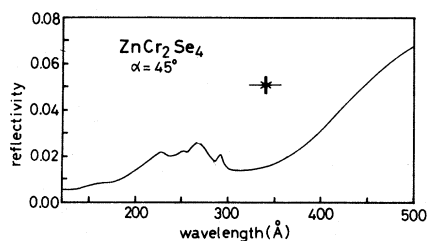


FIG. 1. xuv reflectance spectrum of ZnCr_2Se_4 at room temperature measured for *s*-polarized light at an incidence angle α of 45° . The resolution (1 \AA) is indicated in the figure.

at room temperature. One finds clear multiplet structures ranging from 230 to 290 \AA . Judging from their energy positions, we assign the structures to be resulting from the $3p$ core levels of the Cr ion, and hereafter call them as $M_{2,3}$ transitions. We are able to discern at least four peaks of these transitions in ZnCr_2Se_4 . With respect to the $M_{2,3}$ transitions from Zn ions, we have not observed any obvious structure in the experimental spectrum. The background reflectivity, except for the $M_{2,3}$ structures, gradually increases to a longer wavelength region and continues to the reflectance resulting from the valence bands as shown below.

Figure 2 shows the near-normal incidence vuv reflectance spectrum of ZnCr_2Se_4 for *p* polarization at $\alpha = 22.5^\circ$ measured at liquid-nitrogen temperature. The sample was attached to a cold finger of a cryostat. A spectrum measured at $\alpha = 12^\circ$ is essentially the same as that observed at $\alpha = 22.5^\circ$. The reflectivity drastically decreases below 700 \AA , which has necessitated a grazing-incidence measurement below 500 \AA as shown before. The spectrum at liquid-nitrogen temperature shows structures at 4.52 eV (2743 \AA), 4.70 eV (2638 \AA), 5.10 eV (2432 \AA), 6.36 eV (1950 \AA), 8.15 eV (1521 \AA), 9.12 eV (1359 \AA), 10.38 eV (1195 \AA), 10.80 eV (1148 \AA), 11.28 eV (1099 \AA), 12.75 eV (972 \AA), 13.25 eV (936 \AA), and 15.76 eV (786.5 \AA). With respect to the gross features of the reflectance spectrum, one should remember that the present result is partly similar to those for CdCr_2Se_4 ,⁵ CdIn_2S_4 ,¹⁰ and CrBr_3 .¹¹ The spectrum of ZnCr_2Se_4 at room temperature shows structures similar to the results at liquid-nitrogen temperature. The intensity of the peak at 6.36 eV , however, decreases considerably at room temperature. In addition, the reflectance peaks at 8.15 and 9.12 eV shift to 7.96 and 8.96 eV , respectively, at room temperature.

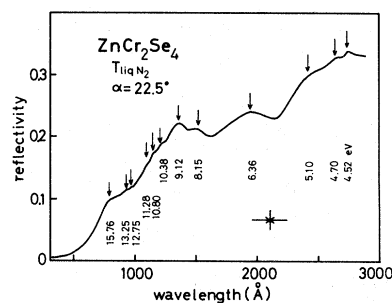


FIG. 2. vuv reflectance spectrum of ZnCr_2Se_4 at liquid-nitrogen temperature for *p*-polarized light at $\alpha = 22.5^\circ$. The resolution (4 \AA) is indicated in the figure.

IV. DISCUSSION

As is well known ZnCr_2Se_4 has a normal spinel structure with Cr ions occupying octahedral sites, each of which is surrounded by six Se ions. On the other hand, the Zn ions are in tetrahedral anionic interstices. As for the valence of the constituent ions, we consider definite valences as Zn^{2+} , Cr^{3+} , and Se^{2-} with Zn^{2+} and Cr^{3+} having $3p^63d^{10}$ and $3p^63d^3$ configurations, respectively, irrespective of a discussion of the valence of Cu in CuCr_2X_4 .^{1,12}

First, we consider that the observed $M_{2,3}$ multiplet structures are due to the transitions from the $3p^63d^3$ ground states to the $3p^53d^4$ final states of the Cr^{3+} ion in analogy with the results for the transition-metal perovskites.¹³ These transitions are represented as $\tilde{d}^7 \rightarrow \tilde{p}\tilde{d}^6$ in the complementary state representation. Since the $3d$ electron states of Cr^{3+} in ZnCr_2Se_4 are split into t_{2g} and e_g conventional molecular orbitals by the cubic crystal field ($10Dq$), the ground states of the Cr^{3+} are described by $|\tilde{t}_{2g}^3\tilde{e}_g^4(^4A_{2g})\rangle$. By use of the coefficients of fractional parentage (CFP) and transformation matrices, the ground states are decomposed into

$$\begin{aligned} & \frac{1}{\sqrt{2}} |\tilde{t}_{2g}, \tilde{t}_{2g}^2(^3T_{1g})\tilde{e}_g^4(^1A_{1g})^3T_{1g}, ^4A_{2g}\rangle \\ & + \frac{\sqrt{5}}{4} |\tilde{e}_g, \tilde{t}_{2g}^3(^4A_{2g})\tilde{e}_g^3(^2E_g)^5E_g, ^4A_{2g}\rangle \\ & + \frac{\sqrt{3}}{4} |\tilde{e}_g, \tilde{t}_{2g}^3(^4A_{2g})\tilde{e}_g^3(^2E_g)^3E_g, ^4A_{2g}\rangle. \end{aligned} \quad (1)$$

Here we neglected the spin-orbit interaction of the d electron and assumed that all the sublevels of the $|\tilde{t}_{2g}^3\tilde{e}_g^4(^4A_{2g})\rangle$ are equally populated.¹⁴ As for the excited states $\tilde{p}\tilde{d}^N$, a detailed description is given elsewhere.¹⁴ An exact calculation of the term energies is performed for such $\tilde{t}_{1u}\tilde{t}_{2g}^n\tilde{e}_g^{N-n}$ system. Since we are concerned with the absorption spectrum, we consider a distribution of the transition intensities from the initial state (1) to the following final states:

$$|\tilde{t}_{1u}, \tilde{t}_{2g}^2(^3T_{1g})\tilde{e}_g^4(^1A_{1g})^3T_{1g}, ^4T_{2u}\Gamma_J\rangle, \quad (2)$$

$$|\tilde{t}_{1u}, \tilde{t}_{2g}^3(^4A_{2g})\tilde{e}_g^3(^2E_g)^5E_g, ^4T_{2u}\Gamma_J\rangle, \quad (3)$$

and

$$|\tilde{t}_{1u}, \tilde{t}_{2g}^3(^4A_{2g})\tilde{e}_g^3(^2E_g)^3E_g, ^4T_{2u}\Gamma_J\rangle. \quad (4)$$

These states correspond to the first, second, and last terms of Eq. (1) as a result of dipole-allowed transitions. The final states other than $^4T_{2u}$ are dipole forbidden as one can recognize from a direct

product of A_{2g} and T_{1u} , which equals T_{2u} , where T_{1u} represents the dipole moment. Γ_J thus obtained are represented by $E_{1u} + E_{2u} + 2G_u$.

For the calculation of term energies, we have considered the spin-orbit splitting of the $3p$ hole (ζ_{3p}) and Coulomb and exchange interactions between p and d electrons (Slater-Condon parameters F_2 and $G_{1,3}$) and between d electrons (Racah parameters B and C) in addition to $10Dq$. Considering that e_g orbitals have more covalency than t_{2g} orbitals with the surrounding anions in a cubic crystal field, we have employed a fitting parameter ϵ for the ratio of the dipole matrix element:

$$\langle t_{1u} || p || e_g \rangle / \langle t_{1u} || p || t_{2g} \rangle.$$

The solid vertical lines in Fig. 3 demonstrate the distribution of eigenenergies and oscillator strengths of the multiplets calculated for the parameters given in Table I and for $\epsilon=0.8$. The parameters B and C are taken from the values in the initial $3p^63d^3$ system¹⁵ and ζ_{3p} is assumed to be the same as that of a free ion.¹⁶ The Slater-Condon parameters and $10Dq$ are evaluated so as to provide a best-fit result for the experimental spectrum. For purposes of comparison, we have further calculated the spectrum by assuming a Gaussian line shape with a full width at half maximum (FWHM) of 1.0 eV for each component of the multiplets as shown by the dashed curve in Fig. 3. The solid curve in Fig. 3 shows the dispersion of the dielectric constant ϵ_2 evaluated from the grazing-incidence reflectance spectrum by assuming the refractive index n as 1.0. The proximity of n to 1.0 is generally known in the core excitation region of solids. The experimental spectrum is thus well reproduced with respect to the peak

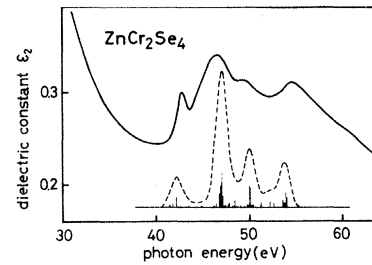


FIG. 3. ϵ_2 (dielectric constant) spectra of ZnCr_2Se_4 in the $M_{2,3}$ inner-core transition region. The solid curve shows the experimental spectrum which is compared with the calculated spectrum (dashed curve) obtained for the parameters given in Table I and $\epsilon=0.8$. The solid vertical lines show the distribution of the bare multiplets calculated on the basis of a ligand-field theory. The ordinate applies only to the experimental spectrum.

TABLE I. Final-state interactions for the $M_{2,3}$ inner-core excitation of Cr^{3+} in ZnCr_2Se_4 . The spin-orbit splitting of the $3p$ hole (ζ_{3p}), cubic crystal field ($10Dq$), Racah parameters (B and C), and Slater-Condon parameters (F_2 , G_1 , and G_3) are given in eV. The reduction factors of F_2 and $G_{1,3}$ from those of the free ion are evaluated as $\kappa_F=0.6$ and $\kappa_G=0.5$, respectively.

ζ_{3p}	0.78 eV
$10Dq$	2.13
B	0.114
C	0.512
F_2 ($3p, 3d$)	0.201
G_1 ($3p, 3d$)	0.487
G_3 ($3p, 3d$)	0.055

energies and relative intensities by the parameters shown in Table I, where $10Dq=2.1$ eV is found to be equal to the corresponding value in the initial $3p^6 3d^3$ state. Meanwhile, the reduction factors κ_F and κ_G of the Slater-Condon parameters F_2 and $G_{1,3}$ from those of the free ion are evaluated as 0.6 and 0.5, respectively. The parameter ϵ is taken as 0.8 in order to explain the relative intensity of the lowest energy peak. The reduction of the Slater-Condon parameters in compounds is due to the covalency effect between the transition-metal $3d$ orbitals (Cr) and anion p orbitals (Se $4p$). A difference of the reduction factors for e_g and t_{2g} orbitals is, however, neglected for simplicity. Remembering that the evaluated κ_F and κ_G in ZnCr_2Se_4 are less than the corresponding values 0.7 and 0.6 of the KMnF_3 (M represents Mn or Co) perovskites,¹³ we interpret that ZnCr_2Se_4 is more covalent than perovskites. This result is reasonable when we consider that ZnCr_2Se_4 is a semiconductor, whereas KMnF_3 are insulators with large band-gap energies of more than 10 eV.

We next move to a discussion of the vuv spectra. Figure 4(a) shows the dielectric constant ϵ_2 and optical constants n and k at liquid-nitrogen temperature. Since the $3d$ levels of Zn^{2+} and the $4s$ level of Se^{2-} are expected more than 10 eV below the bottom of the conduction band according to optical and x-ray photoelectron spectroscopy (XPS) studies of related compounds such as ZnSe ,^{17,18} transitions from these states to conduction bands are the candidates for the reflectance structures at 12.75, 13.25, and 15.76 eV. In pyrites such as FeS_2 , CoS_2 , and NiS_2 ,¹⁹ we have observed a common feature at around 17 eV which has a similar line shape as the 15.76-eV structure in ZnCr_2Se_4 . Considering the difference between S $3s$ and Se $4s$

orbitals, we assign the 15.76-eV structure to the dipole-allowed transition from the Se $4s$ shallow core level. Since the Se^{2-} $4p$ orbitals are hybridized with the $3d$ (e_g) orbitals of the Cr^{3+} due to the covalency as discussed before and also ascertained by band calculations,⁴ the dipole-allowed transition from this Se $4s$ level is expected to the Se $4p$ - Cr $3d$ (e_g) antibonding states, through the intra-atomic channel providing a finite transition intensity. Besides, judging from the fact that Zn $3d$ levels are placed a few eV above the Se $4s$ level in compounds,^{17,18,20} we assign the small structures at 12.75 and 13.25 eV to transitions from the Zn $3d$ levels to the conduction bands having a Zn $4p$ component, or to charge-transfer transitions to the Se $4p$ - Cr $3d$ (e_g) antibonding orbitals. The weak intensities of the observed structures are not inconsistent with both of the two possibilities,

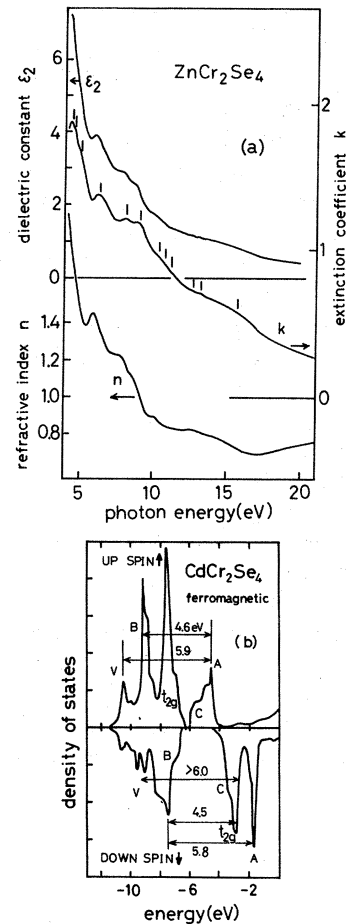


FIG. 4. (a) Dielectric constant (ϵ_2) and optical constants (n, k) of ZnCr_2Se_4 at liquid-nitrogen temperature compared with (b) the density of states of CdCr_2Se_4 (Ref. 4). The vertical lines in (a) show the energy positions of the reflectance structures for comparison.

where the intensity of the former transitions will be limited by the small density of states of the conduction band, irrespective of the intra-atomic nature of the transitions. Further study will be required for a definite assignment of the final states. These doublet structures (12.75 and 13.25 eV) are more clearly resolved by calculating the second energy derivative of the reflectance spectrum. The energy separation of the doublet of about 0.5 eV is considered as due to the splitting of the initial Zn 3*d* states induced by the spin-orbit interaction as well as the T_d crystal field.^{21,18}

With respect to the reflectance structures in the lower photon-energy region below 12 eV, we would like to discuss them in comparison with the results of band calculations. Since both Zn²⁺ and Cd²⁺ in spinel compounds have 3*d*¹⁰ and 4*d*¹⁰ outermost filled shells, the band structure of ZnCr₂Se₄ is expected to be quite similar to that of CdCr₂Se₄.^{3,4} Although our spectra are measured for the paramagnetic phase, we refer to the result of a DV (discrete variational) $X\alpha$ self-consistent calculation performed for the ferromagnetic phase of CdCr₂Se₄,⁴ since the difference is only due to the long-range spin ordering. Apart from detailed structures, the spectrum in Fig. 4(a) is classified into four groups, namely, structures below 5.5 eV, between 5.5 and 7.5 eV, between 7.5 and 12 eV, and above 12 eV. Since the structures of the last group have been interpreted already, we discuss the remaining structures hereafter. According to the DV- $X\alpha$ calculation, an evaluation of the density of states for spin-up and spin-down bands of CdCr₂Se₄ is given in Fig. 4(b).⁴

We consider that the 3*d*³ electrons of the Cr³⁺ ion occupy the up-spin t_{2g} nonbonding orbitals, whereas the down-spin t_{2g} orbitals remain empty. On the other hand, the e_g orbitals are hybridized considerably with the Se²⁻ 4*p* orbitals due to the covalency, as mentioned before, composing bonding as well as antibonding orbitals. Denoting these bands as *B* (bonding), *A* (antibonding), *C* (conduction band), and *V* (valence band), we expect strong dipole-allowed transitions above 4 eV as follows:

$$\begin{aligned}
 & B\uparrow \rightarrow A\uparrow \text{ at } 4.6 \text{ eV}, \\
 & V\uparrow \rightarrow A\uparrow \text{ at } 5.9 \text{ eV}, \\
 & B\downarrow \rightarrow C\downarrow \text{ or } t_{2g}\downarrow \text{ at } 4.5 \text{ eV}, \\
 & B\downarrow \rightarrow A\downarrow \text{ at } 5.8 \text{ eV}, \\
 & V\downarrow \rightarrow t_{2g}\downarrow \text{ or } C\downarrow \text{ above } 6.0 \text{ eV},
 \end{aligned} \tag{5}$$

besides weak transitions as shown in Fig. 4(b). Though these results for CdCr₂Se₄ will not be directly applicable to the case of ZnCr₂Se₄, we can reasonably assign the observed structures at 4.52, 4.70, 5.10, and 6.36 eV to the transitions described in (5) as summarized in Table II. With respect to the remaining structures between 7.5 and 12 eV, however, they are not likely to be interpreted by considering only the electronic levels contained in Fig. 4(b). Since the band calculation predicts that the conduction bands are dominated by Cr 4*p* orbitals around 6.5 to 9.5 eV above the top of the valence band in CdCr₂Se₄,⁴ the observed structures at 8.15, 9.12, and 10.38 eV are assigned to the transitions from the bonding as well as t_{2g} orbitals to these conduction bands through intra-atomic channel as Cr 3*d* → Cr 4*p*.

According to this interpretation, the energy splitting 2.2 eV between the two structures at 10.38 and 8.15 eV can be assigned to the splitting between the $t_{2g}\uparrow$ and $B\uparrow$ bands. With respect to the remaining structures at 10.80 and 11.28 eV with weak intensities, further study will be required for their assignment.

V. CONCLUSION

We have analyzed reflectance spectra of a single crystal ZnCr₂Se₄ measured from 3000 to 120 Å.

TABLE II. Assignment of reflectance structures of ZnCr₂Se₄ between 4.5 and 16 eV. See text for the notation of *B*, *A*, *C*, and *V*.

Transition energies (eV)	Initial state	Final state
4.52 } 4.70 }	{ $B\uparrow$ $B\downarrow$	{ $A\uparrow$ $C\downarrow$ or $t_{2g}\downarrow$
5.10 } 6.36 }	{ $V\uparrow$ $B\downarrow$ $V\downarrow$	{ $A\uparrow$ $A\downarrow$ $t_{2g}\downarrow$ or $C\downarrow$
8.15	$t_{2g}\uparrow$	Cr 4 <i>p</i> ↑
9.12	$B\downarrow$	Cr 4 <i>p</i> ↓
10.38	$B\uparrow$	Cr 4 <i>p</i> ↑
10.80		
11.28		
12.75	Zn 3 <i>d</i>	Zn 4 <i>p</i> or charge transfer to <i>A</i>
13.25		
15.76	Se 4 <i>s</i>	<i>A</i>

and elucidated the electronic structures of a spinel compound. As for the $M_{2,3} 3p$ core excitation of the Cr^{3+} ion observed in xuv spectrum, the final-state interactions have been quantitatively evaluated on the basis of ligand-field theory, which we have recently developed in a comprehensive form. The $M_{4,5} 3d$ core excitation of the Zn^{2+} has been unambiguously assigned in the vuv spectrum. In addition, other structures of the vuv reflectance spectrum are interpreted according to a band calculation by taking the covalency effect on the $Cr^{3+} 3d(e_g)$ orbitals into account. Further studies of temperature change of the vuv spectra as well as XPS and ultraviolet photoelectron spectroscopy (UPS) studies of Zn and Cd spinels will provide

fruitful information about their detailed electronic structures.

ACKNOWLEDGMENTS

The authors are much obliged to Professor H. Kanzaki, Professor S. Sugano, and Mr. T. Oguchi for valuable discussions. We would like to acknowledge the support of colleagues of the Synchrotron Radiation Laboratory for the present experiment and for operating SOR-RING. This work was partly supported by a grant-in-aid for Scientific Research (Grant No. 354072) of the Ministry of Education, Science and Culture of Japan.

-
- ¹J. B. Goodenough, *J. Phys. Chem. Solids* **30**, 261 (1969).
²K. Dwight and N. Menyuk, *Phys. Rev.* **163**, 435 (1967).
³T. Kambara, T. Oguchi, and K. Gondaira, *J. Phys. C* **13**, 1493 (1980).
⁴T. Oguchi, T. Kambara, and K. Gondaira, *Phys. Rev. B* **22**, 872 (1980); T. Kambara, T. Oguchi, G. Yokoyama, and K. Gondaira, *Jpn. J. Appl. Phys. Suppl.* **19-3**, 223 (1980).
⁵M. Zvara, V. Prosser, A. Schlegel, and P. Wachter, *J. Magn. Magn. Mater.* **12**, 219 (1979).
⁶S. Nakai, H. Nakamori, A. Tomita, K. Tsutsumi, H. Nakamura, and C. Sugiura, *Phys. Rev. B* **9**, 1870 (1974).
⁷S. Shin, S. Suga, M. Taniguchi, H. Kanzaki, S. Shibuya, and T. Yamaguchi, *J. Phys. Soc. Jpn.* **51**, 906 (1982).
⁸T. Watanabe, S. Endo, and A. Kasai, *Jpn. J. Appl. Phys. Suppl.* **19-3**, 279 (1980).
⁹T. Watanabe and I. Nakada, *Jpn. J. Appl. Phys.* **17**, 1745 (1978).
¹⁰E. Grilli, M. Guzzi, A. Anedda, F. Raga, and A. Serpi, *Solid State Commun.* **27**, 105 (1978).
¹¹G. Guizzetti, L. Nosenzo, I. Pollini, E. Reguzzoni, G. Samoggia, and G. Spinolo, *Phys. Rev. B* **14**, 4622 (1976); S. Antoci and L. Mihich, *ibid.* **18**, 5768 (1978).
¹²J. Hollander, G. Sawatzky, and C. Haas, *Solid State Commun.* **15**, 747 (1974).
¹³S. Shin, S. Suga, H. Kanzaki, S. Shibuya, and T. Yamaguchi, *Solid State Commun.* **38**, 1281 (1981).
¹⁴T. Yamaguchi, S. Shibuya, and S. Sugano, *J. Phys. C* (in press).
¹⁵S. Sugano, Y. Tanabe, and H. Kamimura, *Multiplets of Transition-Metal Ions in Crystals* (Academic, New York, 1970).
¹⁶T. Yamaguchi, S. Shibuya, S. Suga, and S. Shin, *J. Phys. C* (in press).
¹⁷J. L. Freeouf, *Phys. Rev. B* **7**, 3810 (1973).
¹⁸L. Ley, R. A. Pollak, F. R. McFeely, S. P. Kowalczyk, and D. A. Shirley, *Phys. Rev. B* **9**, 600 (1974).
¹⁹S. Suga (unpublished).
²⁰J. C. Rife, R. N. Dexter, P. M. Bridenbaugh, and B. W. Veal, *Phys. Rev. B* **16**, 4491 (1977).
²¹F. J. Himpsel, D. E. Eastman, E. E. Koch, and A. R. Williams, *Phys. Rev. B* **22**, 4604 (1980).